Structural characteristics and lattice distortion of nanocrystalline selenium

Structural characteristics and lattice distortion of nanocrystalline selenium

H Y Zhang†, K Lu‡ and Z Q Hu†

† National Laboratory for RSA, Institute of Metal Research, Academia Sinica, Shenyang 110015, People's Republic of China
‡ International Centre for Materials Physics, Academia Sinica, Shenyang 110015, Peoples's Republic of China

Abstract. Bulk nanocrystalline selenium (nc-Se) samples were prepared by crystallizing as-quenched amorphous selenium (a-Se). The structure of nc-Se was investigated by x-ray diffraction (XRD) and transmission electron microscopy (TEM). nc-Se samples are of trigonal structure with grain sizes ranging from 8.4 to 27.8 nm. Direct TEM observations showed that nc-Se consists of lamellae which are made up of fibres with a nanometre-sized thickness. A lattice distortion was revealed in nc-Se from quantitative XRD measurements, i.e., the lattice parameter a increases and c decreases simultaneously with a reduction in grain size. For the samples with grain sizes smaller than 12 nm, the unit cell volume is expanded; but it is contracted for those with grain sizes larger than 12 nm. A change of elastic modulus with grain size is inferred from the change of unit cell volume.

1. Introduction

Nanocrystalline (nc) materials are defined to be composed of two components including nanometre-sized grains and a large volume fraction of interfaces (Gleiter 1989). This new class of materials has attracted considerable attentions in recent years (Gleiter 1989, Siegel 1993). Many properties of nc materials have been found to be essentially different from those of the conventional polycrystals and the glassy states, which is certainly related to their special microstructural characteristics, especially to the large number of interfaces. However, an important question is actually open as to whether or not the lattice structure is unstable relative to the perfect single crystal when the crystallites are refined down to a few nanometres.

It has been reported in the literature that the crystal structures of ultrafine particles are unstable with respect to the perfect crystal structure, such as in gold particles (Solliard 1981) and the aluminium particles in a sandwich Al/MgO (Woltersdorf *et al* 1981). Schroeer and Nininger (1967) reported that lattice spacing increases with decreasing particle size of α-Fe_2O_3 microcrystals, which results in the depression of the Morin transition temperature of the material. It is imaginable that the structural variations in ultrafine crystallites would affect the properties of nc materials. For example, Vepřek et al (1982) showed that the crystal lattice expansion of microcrystalline silicon film in the crystallite size limit of 3 nm leads to an instability of the diamond structure with respect to the amorphous phase.

Recently, quantitative measurements on lattice parameters of the nanometre-sized intermetallics Ni_3P (Lu and Sui 1993) and Fe_2B (Liu *et al* 1993) nanophases in nc Ni–P and

Fe–Cu–Si–B alloys synthesized by fully crystallizing the amorphous alloys demonstrated that the crystal structure of the nanophases is not perfect but distorted compared to the Ni_3P and Fe_2B perfect crystals. And the degree of lattice distortion increases with a decrease of grain size. In this work, an attempt was made to examine the structural characteristics and its dependence on the grain size for nanocrystalline selenium (nc-Se), which was prepared by crystallizing bulk amorphous selenium (a-Se).

2. Experimental procedures

2.1. Sample preparation

A bulk amorphous selenium sample with a size of $200 \times 10 \times 3$ mm^3 was prepared by means of the melt quenching technique. A commercial polycrystalline selenium sample with the purity of 99.999% was sealed in a vacuum ampoule, then melted at 400 °C for 1 hour and subsequently quenched in water at room temperature. The amorphism of the as-quenched Se specimen was verified by x-ray diffraction.

Nanocrystalline Se samples were produced by isothermal crystallization of the amorphous state, called the 'crystallization method' (Lu *et al* 1991, 1990). Bulk nc-Se specimens with various grain sizes were available by completely crystallizing the amorphous Se sample at temperatures ranging from 107 to 196 °C. The crystallization processes were monitored by a differential scanning calorimeter (DSC-7, Perkin–Elmer) in a flowing argon atmosphere. Only one exothermic peak was identified in the DSC curves related to the crystallization process (Zhang *et al* 1995b). So the transformation occurring from the amorphous to the nc-Se state may be regarded as a one-step crystallization process.

2.2. Structure characterization

The selected area electron diffraction (SAED) and morphology observations on the crystallized samples were performed on a JEM200cx transmission electron microscope with an accelerating voltage of 200 kV.

Quantitative XRD experiments were performed on a Rigaku x-ray diffractometer, Dmax-rA, with Cu Kα radiation. In order to exactly determine grain size and lattice parameters of nc-Se samples, the samples were ground into powders, in which silicon standard powders were mixed up for calibration. The diffraction line breadth was determined by using the method of full width at half maximum. The separation of Cu Kα_1 and Cu Kα_2 as well as the determination of the peak position and line breadth was carried out automatically on a computer.

3. Results and discussion

3.1. TEM observations

The scanning electron microscopy observation (Zhang *et al* 1995b) reveals that the crystallization product of amorphous selenium is the form of spherulites which are composed of radially oriented lamellae crystals. The detailed substructure of the lamellae was further explored by means of TEM. Figure 1 shows the typical TEM micrographs and the corresponding SAED pattern of an nc-Se sample. As shown in figure 1(a), some lamellae were detected, which are made up of fibres with similar dimensions in width and thickness. Figure 1(b) is a higher-magnification view of a region corresponding to figure

1(a). Clearly, the fibres are about 20 nm in width, and the thickness (or width) of the fibres is nearly the same (about 20 nm). Many fibres are found to grow out from the edges of the lamellae. In the dark-field TEM image of figure 1(c), the polycrystals precipitated in the sample are oriented randomly, and the average grain size is estimated to be about 20 nm, which is coincident with the grain size data determined by XRD analysis, as listed in table 1. The SAED pattern shows that the sample has a trigonal structure with polycrystalline characteristics. From these observations, it is concluded that the lamellae of nc-Se consist of polycrystalline trigonal selenium with nanometre-sized grains. The morphology seen in the nc-Se sample is very similar to that of a polymerized poly(*p*-oxybenzoate) (Liu and Geil 1993). They suggested that the uniform thickness implies that the dimension of the nucleus determines the thickness of the whiskers.
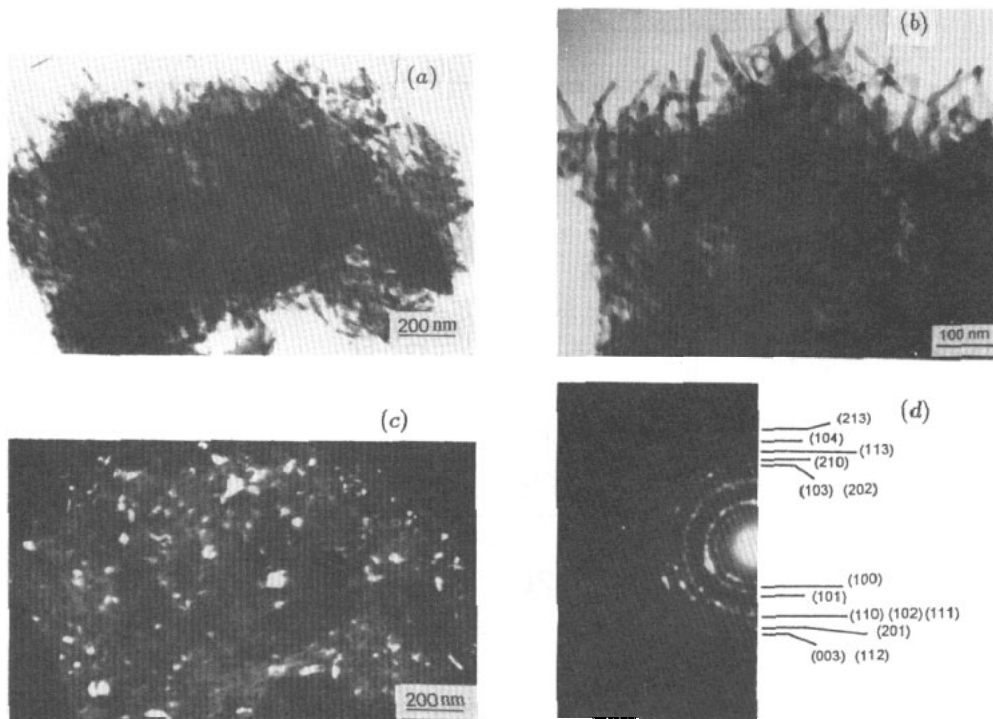

Figure 1. TEM micrographs and corresponding SAED patterns of the nc-Se sample obtained from a-Se annealing at 153 °C for 12 min: (a) bright-field image of TEM, (b) higher magnification view of a region chosen from the image in (a), (c) the corresponding dark-field image of (a), and (d) the corresponding SAED patterns.

3.2. Dependence of lattice parameters on grain size

Figure 2 is the XRD pattern of an nc-Se sample, which confirmed the trigonal structure of the sample. Trigonal selenium with $a_0 = 0.43662$ nm and $c_0 = 0.49536$ nm (Unger and Cherin 1969) is thought of as consisting of helical chains along the c axis , which was proved to be the most stable structure in selenium solids. A series of experimental samples can be obtained by modifying the isothermaly annealing conditions as listed in table 1. As a qualitative analysis, the (104) diffraction line is chosen to calculate the average grain size of the crystallized samples according to the Scherrer equation from the breadth of the x-ray

Table 1. A list of the nanocrystalline selenium samples used in this work. T_a: annealing temperature, t_a: annealing time, D: average grain size normal to (104), a and c: lattice parameters, d_{113}: lattice spacing along (113) zone direction. For the perfect crystal, $a_0 = 0.43662$ nm, $c_0 = 0.49536$ nm, $d_{0,113} = 0.13169$ nm

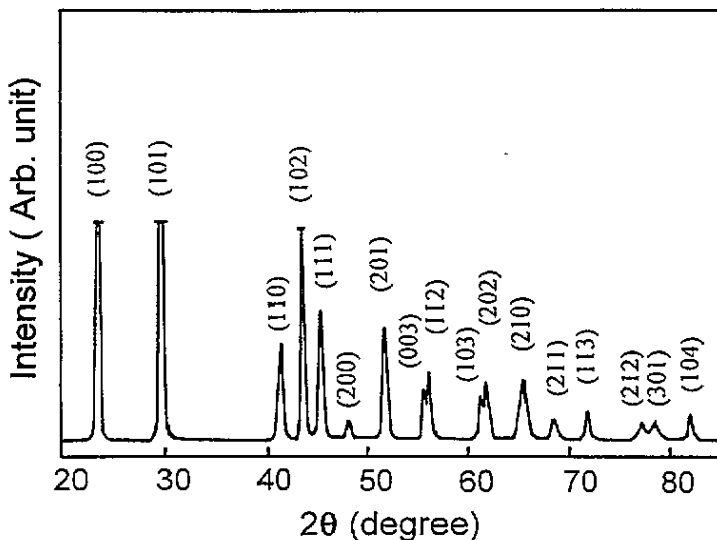| Sample	T_a (°C)	t_a (min)	D (nm)	a (nm)	c (nm)	d_{113} (nm)
A	107	50	8.4	0.43787	0.49442	0.13167
B	117	25	10.4	0.43700	0.49494	0.13166
C	131	22	13.9	0.43634	0.49493	0.13159
D	153	12	18.5	0.43617	0.49546	0.13166
E	160	11	20.0	0.43609	0.49551	0.13166
F	174	7	24.5	0.43618	0.49563	0.13169
G	196	19	27.8	0.43631	0.49578	0.13173

Figure 2. XRD pattern of sample F obtained from a-Se annealing at 174 °C for 7 min.

diffraction line after removing the instrumental broadening. When the annealing temperature increases from 107 °C to 196 °C, average grain size D increases from 8.4 to 27.8 nm. The (210) XRD lines of three samples, A, B and F, are shown in figure 3. Clearly, all the XRD lines are broadened indicating the refinement of Se crystallites, and all the peak positions deviate from the equilibrium value (dashed line). Moreover, the smaller the grain size is, the greater the deviation is.

The lattice parameters a and c of the nc-Se can be quantitatively determined from the peak positions of the (210) line (for determining a) as well as the (003) and (113) lines (for determining c) according to

$$a = \left[\tfrac{4}{3}(h^2 + hk + k^2)\right]^{1/2} \left(1/d^2 - l^2/c^2\right)^{-1/2} \tag{1}$$

$$c = l \left[\frac{1}{d^2} - \frac{4}{3}\left(\frac{h^2 + hk + k^2}{a^2}\right)\right]^{-1/2} \tag{2}$$

where $d = \lambda/2 \sin\theta$, d is the lattice spacing, λ the wavelength of the radiation.
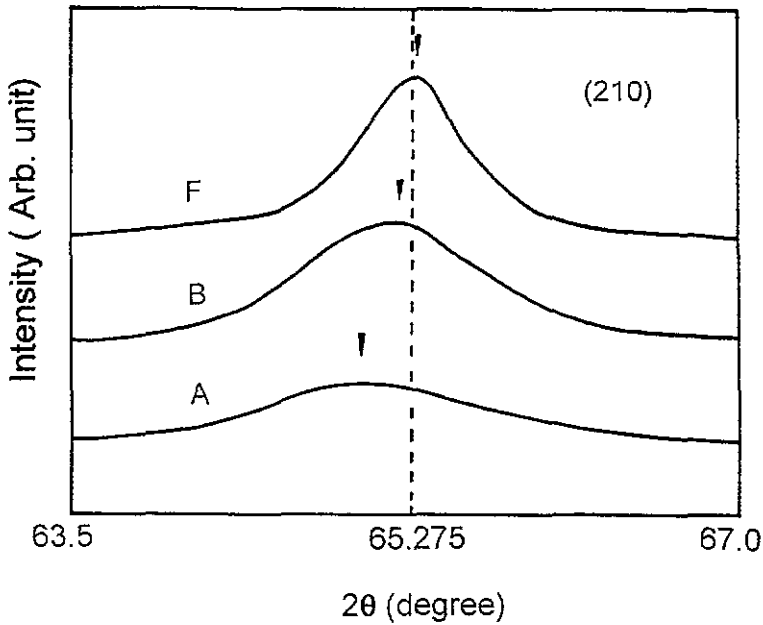
Figure 3. (210) XRD lines of nc-Se samples A, B and F. The annealing conditions are listed in table 1. The dashed line is the peak position of the (210) XRD line for perfect trigonal selenium.

Table 1 lists the measurement results of a and c for nc-Se specimens. According to the instrumental accuracy for determining 2θ ($\Delta 2\theta < 0.02$), the relative error of the data for a and c in table 1 is below 0.05%. It is clear that lattice parameters a and c vary significantly with the grain size of nc-Se, i.e., a increases and c decreases simultaneously with a reduction of grain size. We have used $\Delta a/a_0$ ($\Delta a = a - a_0$, $a_0 = 0.436\,62$ nm) and $\Delta c/c_0$ ($\Delta c = c - c_0$, $c_0 = 0.495\,36$ nm) to represent the departure of the lattice parameters of nc-Se samples from the equilibrium values. The calculated results are summarized in figure 4. As may be seen in figure 4, Δa increases from negative to positive, whereas Δc declines from positive to negative with decreasing average grain size. The variations of Δa and Δc are rather remarkable when grain size is smaller than 15 nm. For sample A with $D = 8.4$ nm, $\Delta a/a_0$ is as much as 0.29% and $\Delta c/c_0$ is -0.19%. For the samples with grain size smaller than 15 nm, the data of c_{003} could not be obtained due to the difficulties in separating the (003) and (112) XRD lines accurately.

Based on the lattice parameters in table 1, unit cell volume change, $\Delta V/V_0$ ($\Delta V = V - V_0$), can be calculated using the formula of $V = (3\sqrt{3}/2)a^2c$, where V_0 is the unit cell volume of a perfect selenium crystal. Unit cell volume change as a function of grain size D is shown in figure 5. Evidently, unit cell volume varies dramatically with grain size of nc-Se. When D is less than 15 nm, $\Delta V/V_0$ decreases with increasing grain size. When D is larger than 15 nm, $\Delta V/V_0$ increases and unit cell volume tends to the value V_0 with an increase of grain size. Clearly, the grain size value of 15 nm corresponds to the inflexion point in $\Delta V/V_0 \sim D$ plot. Moreover, it can be seen that for the samples with grain size below about 12 nm, the unit cell volume change is positive, indicating an expanded unit cell, and the largest expansion is obtained at $D = 8.4$ nm, which is 0.36%. It is also noticeable that, for the samples with grain size larger than 12 nm, unit cell volume changes are negative, implying that the crystal lattice of nc-Se is contracted at that time. The maximum lattice contraction reaches 0.2% at $D = 13.9$ nm.
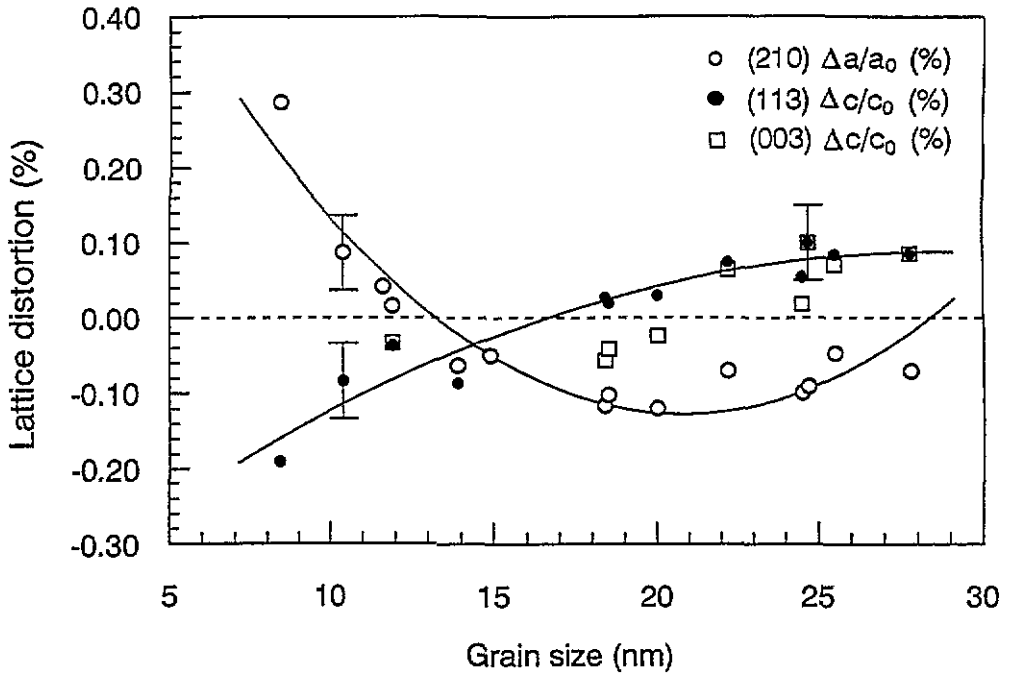
Figure 4. Variation of lattice distortions $\Delta a/a_0$ and $\Delta c/c_0$ with grain size.
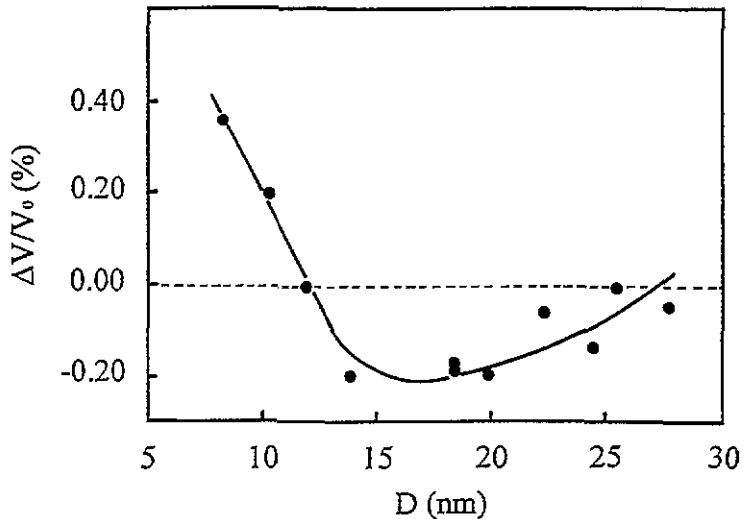

Figure 5. Relationship between unit cell volume change $\Delta V/V_0$ and grain size.

It can be inferred that the changes in lattice parameters with grain size could lead to a change in elastic modulus with grain size. Elastic modulus may be approximately expressed as a function of atom distance. On the assumption that a change in atom distance with grain size is consistent with unit cell volume change, it would be obtained that elastic modulus increases with grain size to the inflexion point, then decreases. The change of elastic modulus with grain size may be confirmed by the relationship between microhardness and

grain size (Zhang *et al* 1995a). Therefore, the lattice distortion in nc materials may play an important role in the microstructure characteristics and in the properties of nc materials as well.

According to the evidence presented above, we find that the lattice parameters of nc-Se change with grain size, i.e. lattice parameter a elongates with a reduction of grain size, whereas the value of c declines. Similar results have been found in nanophase Ni_3P (Lu and Sui 1993) and Fe_2B (Liu and Sui 1993) (both have a body-centred tetragonal structure, bct). Lu *et al* (1993) explained the lattice distortion in nc materials according to thermodynamic considerations. With respect to that of the infinite large crystal, the free energy of a crystallite, of which the dimension is D, will be enhanced by

$$\Delta G(T, D) = 4\Omega\gamma/D \tag{3}$$

where Ω is the atomic volume of the grain and γ is the interfacial free energy. From this point of view, a reduction of grain size will enlarge the free energy of the crystallites and then raise the equilibrium solute solubility in the crystal lattice. In a pure element system, point defects and vacancies are the possible 'solute atom'. The solutions in the crystal lattice will disturb the lattice structure resulting in an lattice expansion, for example, in as-sputtered nc-Ni film (Liu *et al* 1994). However, the case of nc-Se is complex because not only lattice expansion but also lattice contraction exist in crystallized samples. So, it is difficult to explain the lattice distortion of nc-Se only in view of enhanced solubility of vacancies or point defects.

4. Summary

1. Bulk nc-Se samples with grain size D of 8.4–27.8 nm were prepared by crystallizing as- quenched selenium over the temperature range from 107 to 196 °C.

2. Nanocrystalline Se has a lamella structure, which is made up of fibres with random orientations. The dimensions of the fibres are uniform in width and thickness.

3. An evident lattice distortion was obtained in nc-Se. Parameter a is enlarged and c is reduced simultaneously with decreasing grain size. The maximum lattice expansion amounts to 0.36% and the largest lattice contraction of nc-Se to −0.2%.

Acknowledgments

References

Gleiter H 1989 *Prog. Mater. Sci.* **33** 223–315
Liu J and Geil P H 1993 *Polymer* **34** 1366–74
Liu X D, Lu K, Ding B Z and Hu Z Q 1993 *Nanostruct. Mater.* **2** 581–6
Liu X D, Zhang H Y, Lu K, and Hu Z Q 1994 *J. Phys.: Condens. Matter* **6** L497–502
Lu K and Sui M L 1993 *J. Mater. Sci. Technol.* **9** 419–22
Lu K, Wang J D and Wei W D 1990 *Scr. Metall. Mater.* **24** 2319–23
——1991 *J. Appl. Phys.* **69** 522–4
Schroeer D and Nininger R C Jr 1967 *Phys. Rev. Lett.* **19** 632–4
Siegel R W 1993 *Mater. Sci. Eng.* A **168** 189–97
Solliard C 1981 *Surf. Sci.* **106** 58–63
Unger P and Cherin P 1969 *The Physics of Selenium and Tellurium* ed W C Cooper (Oxford: Pergamon) pp 223–9

Vepřek S, Iqbal Z and Sarott F A 1982 *Phil. Mag.* B **45** 137–45
Woltersdorf J, Nepijko A S and Pippel E 1981 *Surf. Sci.* **106** 64–9
Zhang H Y, Hu Z Q and Lu K 1995a *J. Appl. Phys.* at press
——1995b *Nanostruct. Mater.* **5** 41–57